

THE RELATION BETWEEN CHEMICAL ENRICHMENT AND CORE MASS IN PLANETARY NEBULAE

JAMES B. KALER

Department of Astronomy, University of Illinois

AND

GEORGE H. JACOBY

Kitt Peak National Observatory, National Optical Astronomy Observatories¹

Received 1990 February 15; accepted 1990 April 17

ABSTRACT

From innovative methods of analysis applied to data on planetary nebulae in the Magellanic Clouds, we derive the masses of 32 central stars, the nebular nitrogen and helium abundances, and the form of the relationships among these properties. We find that N/O stays relatively constant at about 0.2 from the lowest core mass up to about $0.65 M_{\odot}$, whereupon it climbs very suddenly to high levels, between 1 and 2, by $0.7 M_{\odot}$. Above $0.9 M_{\odot}$, N/O either stays constant with increasing core mass or even declines, but it does not continue to increase. The relation is similar to that seen for the Galaxy by Kaler, Shaw, and Kwitter, but is much tighter since the distances to planetaries in the Clouds are much better known. We also see a continuous increase of He/H with core mass for masses below $0.8 M_{\odot}$. The almost discontinuous increase of N/O, which appears correlated with a drop in C/O, cannot be explained by ordinary dredge-up processes but can be understood by invoking envelope-burning. Our results provide powerful input for improvement of stellar theories and for the understanding of chemical enrichment in the envelopes of giants and in galaxies.

Subject headings: galaxies: Magellanic Clouds — nebulae: abundances — nebulae: planetary — stars: evolution

I. INTRODUCTION

Planetary nebulae, as has been amply demonstrated over the past two decades, reflect the evolutionary histories of the giant stars that preceded them, and carry the by-products of nuclear burning—enriched levels of helium, nitrogen, and carbon—back into interstellar space from whence the stars came. They are therefore part of the chain by which galaxies chemically evolve. Nearly twenty years ago Peimbert and Torres-Peimbert (1971) announced that planetaries as a whole are enriched by about a factor of 4 in nitrogen as a result of contamination of the gas by CNO-burning. Danziger, Frogel, and Persson (1973), Aller *et al.* (1973), and Kaler (1974) subsequently found that these nebulae could be enriched in helium as well, and that high helium abundances were not just an artifact of photographic measurements. Aller (1976) confirmed the nitrogen enrichments and found that the nitrogen content of Greig's (1971, 1972) B-type objects—which tend strongly to the galactic plane—is selectively elevated. Barker (1978) further confirmed nitrogen and helium overabundances. Then Peimbert (1978) divided the nebulae into four composition groups of which his Type I, defined as having $\text{He}/\text{H} \geq 0.14$ and a high nitrogen abundance, was tied to Population I and thereby to more massive progenitors. Finally, the continuous correlation of the nitrogen and helium enrichments was elucidated by Kaler, Iben, and Becker (1978), who showed a reasonable fit with dredge-up theory for giant stars. Torres-Peimbert and Peimbert (1978) concluded that carbon could also be overabundant in planetary shells, although the suspicion goes all

the way back to Aller and Menzel (1945). Some analyses of *IUE* data for a time suggested that the observed carbon enrichments were due simply to problems with interpreting the optical observations (see Kaler 1981 for a brief review), but it is now generally concluded that carbon can indeed be high. The theory of the upward dredging of these three elements in giants was developed by Becker and Iben (1979, 1980) and Renzini and Voli (1981). Broad overviews of the subject are given by Aller (1984), Pottasch (1984), Kaler (1985*a*), and Clegg (1989).

In spite of some initial success, however, the observations do not agree that well with theory. Very high nitrogen abundances, with N/O well over unity, are not predicted by Becker and Iben (1980) (in part because of observational constraints imposed by carbon abundances), and Renzini and Voli's (1981) "hot bottom (envelope) burning" must be invoked to explain them. The highest He/H ratios, up to 0.2 or so, are not explained by anyone, and the observed relation between C/O and He/H fits the theory quite poorly.

A different approach to the problem was taken by Kaler, Shaw, and Kwitter (1989, 1990), hereafter KSK. Kaler (1983) showed that for large planetaries—those with stars on descending, or cooling, evolutionary tracks—high N/O tended toward higher core mass (M_c) in qualitative accord with theory and with the prediction made by Renzini (1979). KSK, then, in a much more extensive study of large nebulae, derived core masses by placing the stars on the ($\log L$ - $\log T$)-plane relative to a set of evolutionary tracks, and for the first time actually established a relation between M_c and nebular N/O. They found that as M_c increases from a low of $0.55 M_{\odot}$ that N/O first stays constant at about twice solar until about $M_c \approx 0.8$. Beyond that N/O is high, reaching values of the order of 2. This behavior is counter to the steady upward progression suggested by Becker and Iben (1980), whose theory does not

¹ The National Optical Astronomy Observatories are operated by the Association of Universities for Research in Astronomy, Inc., under cooperative agreement with the National Science Foundation.

predict N/O beyond unity. Kaler and Jacoby (1989), hereafter KJ, confirmed the large increase with core mass by showing that N/O and central star temperature (T_*) are positively correlated for optically thick nebulae. These objects have stars that are on cooling tracks, and on the average T_* is directly correlated with M_c .

Both of these analyses are crude, however. KSK could only derive distances from the Shklovsky method. Thus the stellar luminosities, hence core masses, are only poorly known, thereby producing considerable dispersion in the N/O – M_c relation, and hiding the true correlation. The N/O – T_* relation from KJ is even more compromised since the M_c – T_* relation changes strongly as a function of stellar luminosity, and the KJ distances and luminosities are all upper limits because of the optically thick nature of the nebulae.

The real purpose of the KJ paper was to establish a reliable way of obtaining central star temperatures for optically thick planetaries. They employed what they termed the “crossover method,” actually Ambartsumyan’s (1932) method, in which T_* is derived from the He II $\lambda 4686/H\beta$ flux ratio. The method works only for optically thick nebulae, however, since all the stellar photons in both the H and He⁺ Lyman continua must be absorbed by the nebular gas. The above flux ratio then gives the ratio of the two Lyman continua, which, for any adopted model (KJ used a blackbody), yields T_* . The term “crossover,” or $T(\text{cross})$ comes from the way in which KJ calculated the temperature. Using a standard Zanstra code, they started with a low hypothetical central star magnitude, which produces $T_z(\text{H}) < T_z(\text{He II})$. They then stepped upward in V until the two temperatures “crossed over” or were equal, which they should be if the nebula is optically thick and the star a blackbody.

There are two problems with this approach. First, the nebulae may not be optically thick and the star may not be a blackbody (the Zanstra discrepancy, $T_z(\text{He II}) > T_z(\text{H})$ is alternatively explained by an ultraviolet excess: see Henry and Shipman 1986 and Mendez *et al.* 1988). KJ introduced two innovations to the original method to treat these difficulties. First, they used an independent spectroscopic criterion for optical depth, that the [O II] $\lambda 3727/H\beta$ and/or the [N II] $\lambda 6584/H\alpha$ flux ratios must be greater than unity (the $\lambda 3727/H\beta$ criterion was later raised to 1.5). If ionizing photons escape the nebula, higher ionization will persist to the mass boundary, whereas if optical depth is high, low ionization species will dominate at the periphery; see Kaler (1983). Second, the crossover technique allows the prediction of a central star magnitude that can be checked against observation, allowing for a critical test of the method and of the optical depth criterion. KJ showed reasonable agreement between $V(\text{cross})$ and $V(\text{obs})$, and in a more stringent test, Jacoby and Kaler (1989) showed excellent agreement between the two, with a dispersion of only 0.5 magnitudes.

Thus the method seems to work very well, allowing for the determination of T_* in optically thick nebulae for which the central star is unobservable. In this paper we turn the technique to the planetaries of the Magellanic Clouds, in which the nebulae are too small, usually unresolvable, and the stars too faint, to allow for simple (or *any*) determination of magnitude. Then, since the distances are securely known, we can derive much more accurate core masses from placement of the stars on the ($\log L - \log T$)-plane. Improved analysis of nebular data then produces more accurate N/O ratios, allowing us finally to establish—at least in part—the form of the N/O – M_c relation.

II. TEMPERATURES, LUMINOSITIES, AND CORE MASSES OF MAGELLANIC CLOUD PLANETARY NEBULAE

The first step is to define a criterion for optical depth for the Magellanic Cloud (MC) planetaries. Both KJ and Jacoby and Kaler (1989) finally recommended that the global [O II] $\lambda 3727$ strength be 1.5 times that of $H\beta$. However, the Clouds have a lower oxygen abundance than does the Galaxy, so that this critical ratio will also be lower. From Pagel *et al.* (1978) and Dufour, Shields, and Talbot (1982), O/H for the LMC and SMC are 2.4×1.1 and 1.04×10^{-4} , respectively, and from Kaler (1980), O/H for disk planetaries averages 4.5×10^{-4} . If we scale the above conservative galactic criterion for optical depth according to these oxygen ratios, we obtain $I([\text{O II}] \lambda 3727) = 80$ and 35 [on the scale $I(H\beta) = 100$] for the LMC and SMC, respectively. However, as O/H declines, the electron temperature must increase, which will increase the $\lambda 3727$ strength. With the typical Cloud temperatures adopted in the next section, the critical values would respectively rise to 120 and 75 for the Large and Small Clouds. We adopt the most liberal (lowest) values for now in order to maximize the sample size, and discuss the results later. We do not use the nitrogen criterion [$I([\text{N II}] \lambda 6584)/I(H\alpha) > 1$] used initially by KJ, both for simplicity and because the nitrogen abundances are so subject to unknown enrichments.

The next step was a search in the literature of relative intensities of MC planetaries so as to find those with sufficiently strong [O II] lines. The principal surveys are by Monk, Barlow, and Clegg (1988), hereafter MBC, and Boroson and Liebert (1989), hereafter BL, to which we add the older and/or more limited observations by Osmer (1976), Webster (1969, 1976), Dufour and Killen (1977), Aller *et al.* (1981), Aller (1983), Dopita, Ford, and Webster (1985), and Peña and Ruiz (1988). We give the final list of objects in Table 1, with the names of the nebulae in column (1) and the $\lambda 3727$ intensities [for $I(H\beta) = 100$ and corrected for reddening, to be discussed below] in column (2).

The names of the MC nebulae are a perpetual problem. Some carry several from different discovery lists. Worse yet, the important Westerlund and Smith (1964) objects are known as “WS” in some papers and “P” in others. Sanduleak, MacConnell, and Philip (1978) ordered the chaos with new comprehensive running numbers and a cross-list of discovery names. Jacoby (1980) then added an extensive catalog of newly discovered fainter objects. Between the two catalogs all or most of the MC planetaries are covered. We preferentially use the Jacoby numbers (called SMC and LMC in accord with previous practice), then the SMP numbers, but present the SMP objects first in Table 1 since they are generally the brighter ones.

In order to derive the temperatures and luminosities of the central stars (T_* and L_*) by the crossover method we must have the following data: the ratios of He II $\lambda 4686$ fluxes to those of $H\beta$, rather the relative intensities of $\lambda 4686$; the extinction constants; and the total $H\beta$ fluxes. These three quantities are presented in columns (3), (4), and (6) of Table 1, where the He II intensities are on the scale $I(H\beta) = 100$, and both these and the $H\beta$ fluxes are corrected for reddening. References to the He II and $H\beta$ data are given in columns (5) and (7), respectively. The MBC (and some other) data are published as already corrected for interstellar extinction. For the remainder, including all the BL data, we corrected the intensities of $\lambda 3727$ and $\lambda 4686$ via the Whitford (1958) reddening function and the

TABLE 1
EVOLUTIONARY PARAMETERS OF MAGELLANIC CLOUD PLANETARY NEBULAE

Nebula (1)	$I_c(\lambda 3727)^a$ (2)	$I_c(\lambda 4686)^a$ (3)	c^b (4)	Reference (5)	$-\log F(H\beta)^a$ (6)	Reference (7)	V_c^a (8)	$10^3 T_*$ (9)	L_*/L_\odot (10)	M_c (11)
LMC										
SMP 7 ^c	279	68	(0.21)	1	12.93	2	23.91	222	1750	0.74
SMP 15	97	27	(0.21)	1	12.47	2, 3	21.64	137	3510	0.61
SMP 19	157	35	(0.21)	1	12.54	2	22.07	153	3210	0.63
SMP 21	149	59	0.28	1, 4, 5, 6, 7	12.50	2, 3, 4, 6, 7	22.61	201	4330	0.68
SMP 33	175	39	(0.21)	1	12.62	2	22.38	160	2760	0.63
SMP 35	103	19	(0.21)	1	12.61	2, 3	21.69	122	2360	0.59
SMP 37	105	47	(0.21)	1	12.66	2	22.70	176	2700	0.65
SMP 40	265	54	(0.21)	1	13.14	2, 3	24.08	190	950	0.72
SMP 45	142	13	(0.21)	1	12.91	3, 7	22.18	110	1120	0.57
SMP 78	113	28	0.34	1, 5, 7, 8	12.26	2, 3, 4, 7	21.15	139	5730	0.65
SMP 83	92	66	0.14	1, 9, 10	12.53	2, 7	22.86	217	4300	0.70
SMP 93	373	55	(0.21)	1	13.17	2	24.18	192	890	0.73
LMC 4 ^d	312	75	0.05	11	14.03	3	26.84	240	150	1.2
LMC 5	184	43	0.73	11	12.54	2	22.30	168	3430	0.65
LMC 12	419	6	0.21	11	13.96	3	24.27	90	92	0.57
LMC 15	481	7	0.19	11	14.04	11	24.56	93	78	0.59
LMC 16	1128	7	0.40	11	14.14	11	24.82	93	62	0.60
LMC 20	354	48	0.00	11	13.99	3	26.05	178	130	0.96
LMC 22	84	49	0.42	11	14.06	11	26.25	180	109	1.01
LMC 23	532	70	0.42	11	14.02	11	26.69	227	145	1.15
LMC 24	299	22	0.15	11	13.90	11	25.06	128	120	0.70
LMC 32	665	13	0.81	11	13.68	11	24.08	109	190	0.60
LMC 35 ^e	217	64	0.00	11	13.53	3	25.31	212	420	0.90
LMC 38	310	77	0.00	11	13.66	11	25.97	246	355	1.08
SMC										
SMP 5 ^f	73	43	0.00	1, 12	12.83	2, 3, 4, 7	23.02	168	2320	0.64
SMP 14	58	35	(0.12)	1	12.87	2, 3, 7	22.89	152	1980	0.62
SMP 22	75	61	0.07	5, 6	12.81	2, 3, 6	23.43	205	2800	0.69
SMC 1 ^d	50	10	0.00	11	13.62	11	23.74	101	280	0.56
SMC 3 ^f	75	64	0.00	1, 11	13.45	3	25.11	212	670	0.83
SMC 6	169	65	0.29	11	14.37	11	27.43	214	81	1.2
SMC 18	79	27	0.42	11	14.54	11	26.82	137	39	0.93
SMC 27	261	9	0.39	11	14.50	11	25.88	99	36	0.68

REFERENCES.—(1) Monk, Barlow, and Clegg 1988; (2) Meatheringham, Dopita, and Morgan 1988; (3) Wood *et al.* 1987; (4) Aller 1983; (5) Dufour and Killen 1977; (6) Osmer 1976; (7) Webster 1969, 1983; (8) Webster 1976; (9) Dopita, Ford, and Webster 1985; (10) Peña and Ruiz 1988; (11) Boroson and Liebert 1989; (12) Aller *et al.* 1981.

^a All data and results (including V) corrected for interstellar reddening.

^b Values in parentheses are the means for the LMC and SMC.

^c SMP numbers from Sanduleak, MacConnell, and Philips 1978.

^d LMC, SMC numbers from Jacoby 1980.

^e SMP 54.

^f SMP 9.

extinction constant, c (the logarithmic extinction at $H\beta$), as determined from the observed $H\alpha/H\beta$ intensity ratio. In cases where no extinction could be found we adopted a mean of 0.21 for the LMC as derived from BL, Osmer (1976), and Dufour and Killen (1977), and 0.12 for the SMC as found from BL and Aller *et al.* (1981).

The absolute fluxes present another problem. Those from Wood *et al.* (1987) and Meatheringham, Dopita, and Morgan (1988) are not corrected for the nebular or stellar continuum. However, they generally scale well to the Webster (1969, 1983) fluxes, which *are* so corrected, and except for isolated cases where there may be a bright central star—none of which would be expected for our sample—they appear to be accurate. In turn, the galactic Webster (1969, 1983) fluxes have been examined by Shaw and Kaler (1989) and also appear to be quite accurate. The BL fluxes are another matter, and seem to suffer from systematic and random error. In Figure 1 we plot the logarithms of the BL fluxes against the observed log fluxes from the above citations (from which 0.02 was subtracted to

bring them to the modern photometric system: Shaw and Kaler 1989). The BL fluxes are too bright at the high end and seem to converge to better agreement with the test fluxes at the faint end. There are also a trio that fall wide of any correlation: LMC 4, LMC 20, and LMC 35 = SMP 54. It makes no difference in the plot if the Webster fluxes are used alone. We averaged all the fluxes for a particular object, *corrected them for interstellar reddening*, and except for the BL values, again subtracted 0.02 from the corrected $\log F_c(H\beta)$. We consider the BL fluxes to be suspect until confirmed, and use them only in the absence of others; they are all grouped in the LMC and SMC numbers of Table 1.

We then use these data to calculate, via the methodology of KJ, the expected V magnitudes, temperatures, and luminosities of the central stars. For V and L_* we adopt distances of 50.1 ($m - M = 18.5$) and 57.5 ($m - M = 18.8$) kpc for the LMC and SMC respectively, from consideration of the work by Schommer, Olszewski, and Aaronson (1984), Conti, Garmany, and Massey (1986), and Feast and Walker (1987) and references

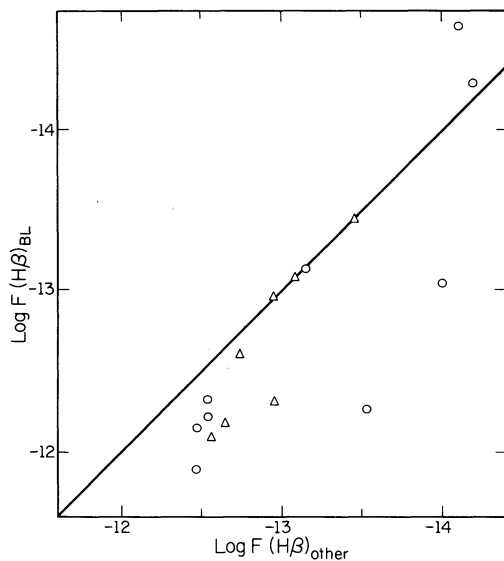


FIG. 1.—Borson and Liebert's (1989) observed fluxes plotted against mean fluxes (where appropriate) from Webster (1969), Dopita *et al.* (1988), and Meatheringham, Dopita, and Morgan (1988); circles: LMC; triangles: SMC. The straight line represents perfect agreement.

therein. V and L_* are then derived from the intensity of $\lambda 4686$ and the $H\beta$ flux, and are presented again as corrected for interstellar extinction. In order to estimate the expected observed V add $0.6c$. The T_* are derived strictly from $I(\lambda 4686)$ and are independent of distance. These quantities are listed in columns (8), (9), and (10) of Table 1. Note that typical V magnitudes for these stars are generally 22 to 27. Clearly, most of these stars cannot currently be observed by any direct technique.

It is interesting to compare our results for the LMC/SMC catalog objects with those derived by Henry, Liebert, and Borson (1989). With the exceptions of LMC 5 and LMC 35 our L_* are more-or-less similar. The temperatures are another matter. Inspection of the tables seems to show no relation between ours and theirs, and some huge discrepancies. They derived their temperatures from the Stoy method (Kaler 1976; Preite-Martinez and Pottasch 1983). Given the validity of the crossover method, which has been carefully verified with galactic planetaries, we conclude that the Stoy method as it is presently applied to higher excitation nebulae (those with He II lines) simply does not work.

With the T_* and L_* known, we can now derive a significantly large set of core masses (M_c) from theoretical evolutionary tracks. The central stars of the objects of Table 1 are plotted on the $(\log L - \log T)$ -plane in Figure 2, where the LMC and SMC nuclei are respectively indicated by circles and triangles; if L_* is derived from a BL flux, the symbol is filled. Note that the BL stars are *much* fainter than the others (seen also in the V magnitudes of Table 1) as expected from their membership in the Jacoby (1980) list. The evolutionary tracks in Figure 2 are taken from Schönberner and Weidemann (1981) for a core mass of $0.55 M_\odot$, from Wood and Faulkner (1986) for $0.6, 0.7, 0.76, 0.89 M_\odot$ ($\phi = 0.5$, mass loss case A), and from Paczyński (1971) for $1.2 M_\odot$. The core masses, presented in the last column of Table 1, are then found by interpolation. Note the wide range in the Table and in the figure, and that all are either on descending tracks or near the knees of the curves, typical of higher excitation optically thick objects

(see KJ). The wide spread for the fainter BL objects is likely a result of evolutionary time scales.

The errors in these core masses derive from six sources: errors in $I(\lambda 4686)$ and $F(H\beta)$, uncertainty in distance, leakage of radiation that may make a particular nebula less than optically thick, possible deviations in the UV flux spectrum from a blackbody, and improper selection, or mispositionings, of evolutionary tracks. The latter are dependent upon ϕ , the point between shell flashes at which a nebula is ejected, and mass loss that continues into the planetary state. The differences for $\phi = 0.25, 0.5$, and 0.75 are slight, and in view of other errors insignificant. If case B mass loss is assumed, the core masses ought to be lowered by the order of 0.05 , and if $\phi = 0$, they are to be raised by crudely a like amount if the stars are in the region of helium-burning. There is little we can do about this except to accept a self-consistent set; at least the relative core masses should be correct. KJ and Jacoby and Kaler (1989) consider the problem of optical depth and deviations from a blackbody, and conclude that for this set of objects they do not seem to be particular problems; keep in mind, though, that any nebula could be deviant. We have also adopted a fairly conservative depth criterion, and believe the objects to be thick, but again, any individual may leak ionizing radiation if uneven structure allows it; we have no way of judging the error, except to note that a systematically high temperature would be derived in those cases. We can at least estimate errors for the other three sources. Assuming a common (actually somewhat large) error of ± 0.05 in $\log F(H\beta)$ (excluding those from BL) and a rather typical error of $\pm 10\%$ in $I(\lambda 4686)$, the errors in $\log T$ and $\log L$ would be about ± 0.02 and ± 0.05 , respectively. The uncertainty in the MC distances is perhaps 10% , which produces a systematic error ± 0.08 in $\log L_*$. Also of importance is the dispersion in distance, which is about ± 3 kpc, leading to a random error of ± 0.05 in $\log L_*$. The combination of all observational errors is then ± 0.02 in $\log T_*$ and ± 0.07 in $\log L_*$ for the relative luminosities and ± 0.11 for

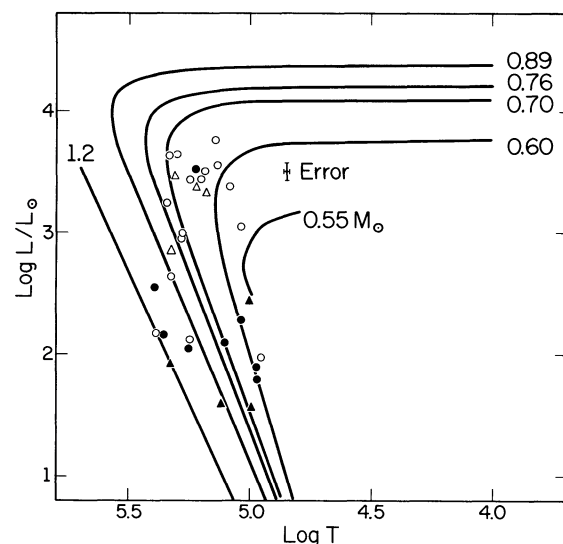


FIG. 2.—The planetary nuclei on the $(\log T)$ -plane. Circles: LMC; triangles: SMC; filled symbols: positions derived from BL fluxes. The evolutionary track for $0.55 M_\odot$ is from Schönberner and Weidemann (1981); for $1.2 M_\odot$ from Paczyński (1971); for the others from Wood and Faulkner (1986) for $\phi = 0.5$, mass-loss case A. The error bars apply to the open symbols; the errors for the closed could be significantly larger.

absolute luminosities. Error bars for the relative values are placed on Figure 2. A 5% error in the *difference* in distance between the two Clouds raises the figures to only ± 0.08 for purposes of comparing core masses in the *LMC* and *SMC*. The resulting errors in core mass depend upon just where on the $(\log L - \log T)$ -plane the star falls. Between 0.6 and 0.7 M_{\odot} the error in $\log T$ produces an error in M_c of roughly $\pm 0.01 M_{\odot}$. Near the knees of the curves the errors on relative $\log L_*$ cause about the same effect, and on the descending tracks the error is perhaps $\pm 0.02 M_{\odot}$. At larger core masses the effects are greater because of the compression of the tracks: around ± 0.07 at 1 M_{\odot} . Typically we suggest a relative error of $\pm 0.03 M_{\odot}$ or so. Absolute errors are only somewhat larger. We must, however, be wary of large individual errors in the BL fluxes, as indicated in Figure 1. They could produce errors in L of up to an order of magnitude and errors in core mass of up to 0.3 or so. We can now go on to see how other nebular parameters, particularly chemical compositions, depend on core mass, and through the theory of evolution, on initial mass.

III. CHEMICAL COMPOSITIONS

The calculation of the chemical compositions of planetary nebulae is straightforward and has been discussed extensively

in the literature including that cited here. We follow the procedure of, and use the code described by, Kaler (1985b). References to atomic data are given there. We only summarize procedure here: He/H is derived from $\lambda 4471$, $\lambda 5876$, and $\lambda 6678$ of He I (with the collisional correlations of Clegg 1987) and He II $\lambda 4686$, with $\text{He}/\text{H} = \text{He}^+/\text{H}^+ + \text{He}^{+2}/\text{H}^+$; O/H is derived from [O II] $\lambda 3727$, [O III] $\lambda 4959$ and/or $\lambda 5007$, with $\text{O}/\text{H} = (\text{O}^+/\text{H}^+ + \text{O}^{+2}/\text{H}^+) (1 + \text{He}^{+2}/\text{He}^+)$; and N/O is found from N^+/O^+ . Additional features of the code are that [O III] electron temperatures (used for O^{+2}/H^+ and He/H ratios) are derived from [O III] $\lambda 4363$ using the $\lambda 4363/\text{H}\gamma$ and $\lambda 5007/\text{H}\beta$ ratios, and the N^+/H^+ ratio is from the [N II] $\lambda 6584/\text{H}\alpha$ ratio in order to minimize observational and reddening errors. (The [N II] electron temperature is, as usual, used for the low ionization species O^+ and N^+).

The data—relative line intensities corrected for interstellar reddening as described above—are taken from the citations of column (5) of Table 1. Each source is reduced independently (with some borrowing from other sources as needed) and the final results averaged for placement in Table 2. The major problem we are faced with is incomplete data, a subject discussed in detail in Kaler (1985). In the present case we quite frequently have no information on the auroral line [N II]

TABLE 2
NEBULAR PARAMETERS AND COMPOSITIONS

Nebulae (1)	T_e [O III] (2)	T_e [N II] (3)	N_e [O II] (4)	N_e [S II] (5)	He ⁺ /H ⁺ (6)	He ⁺² /H ⁺ (7)	10 ⁴ O ⁺ /H ⁺ (8)	10 ⁴ O ⁺² /H ⁺ (9)	He/H (10)	10 ⁴ O/H (11)	N/O (12)	C/O ^a (13)
LMC												
SMP 7	16600	13500	1600	...	0.041	0.064	0.37	1.34	0.105	4.39	1.07	...
SMP 15	11400	(11300)	4600	...	0.055	0.024	0.39	3.07	0.079	4.94	0.13	...
SMP 19	13100	(11300)	2700	...	0.052	0.031	0.46	2.17	0.083	4.18	0.18	...
SMP 21	20400	10700	5100	1700	0.056	0.055	0.50	0.65	0.112	2.36	1.22	0.27
SMP 33	12900	(11300)	4500	13000	0.066	0.034	0.62	2.24	0.101	4.34	0.15	...
SMP 35	12000	(11300)	880	...	0.065	0.017	0.26	2.64	0.082	3.66	0.17	...
SMP 37	13700	10600	7300	...	0.052	0.042	0.53	1.80	0.094	4.20	0.51	...
SMP 40	14000	(11300)	1750	...	0.069	0.049	0.67	1.54	0.119	3.76	0.20	...
SMP 45	14300	(11300)	(200)	...	0.080	0.012	0.32	1.78	0.092	2.41	0.26	...
SMP 78	13400	14500	4400	...	0.700	0.026	0.31	2.08	0.096	3.31	0.22	1.32
SMP 83	15800	11500	2200	1400	0.042	0.061	0.20	0.99	0.103	3.00	0.73	...
SMP 93	15200	11300	(1000)	...	0.093	0.051	0.80	0.57	0.144	2.13	2.18	...
LMC 4	(15500)	(11300)	(100)	0.070	0.57	0.71	2.18	...
LMC 5	21900	(11300)	(3000)	0.041	0.34	0.21	0.65	...
LMC 12	(11300)	(11340)	(200)	0.005	0.99	1.27	...	2.39 ^b	0.13	...
LMC 15	12400	(11300)	(200)	...	0.068	0.006	1.05	1.44	0.075	2.72	0.20	...
LMC 16	(11300)	(11300)	(200)	0.006	2.67	2.24	...	5.4 ^b	0.13	...
LMC 20	17900	(11300)	(1100)	...	0.018	0.045	0.66	0.46	0.093	2.18	1.05	...
LMC 22	(13800)	(11300)	(250)	0.044	0.17	1.59	3.6	...
LMC 23	(15100)	(11300)	(200)	0.065	1.00	1.07	...	7. ^b	0.77	...
LMC 24	20300	(11300)	(200)	0.021	0.42	0.30	...	0.94 ^b	2.22	...
LMC 32	(11500)	(11300)	(200)	0.011	1.55	3.01	...	5.18 ^b	0.24	...
LMC 35	18600	(11300)	(500)	...	0.050	0.061	0.35	0.50	0.111	1.99	2.01	...
LMC 38	16800	(11300)	(300)	...	0.031	0.073	0.54	0.74	0.103	...	1.36	...
SMC												
SMP 5	14200	(12400)	3700	...	0.070	0.037	0.17	1.44	0.106	2.46	0.16	4.3
SMP 14	12400	(12400)	3500	...	0.052	0.031	0.15	1.86	0.083	3.20
SMP 22	(16100) ^c	13300	4300	2500	0.068	0.057	0.15	0.28	0.125	0.78	1.60	0.13
SMC 1	19200	(12400)	(500)	...	0.084	0.009	0.06	0.67	0.094	0.81	0.18	...
SMC 3	12300	(12400)	(1000)	...	0.041	0.058	0.15	2.34	0.098	6.00	0.19	...
SMC 6	(16200)	(12400)	(200)	0.061	0.23	0.18	1.72	...
SMC 18	(13500)	(12400)	(100)	0.024	0.12	0.70	...	1.11 ^b	7.5	...
SMC 27	(12400)	(12400)	(100)	0.008	0.43	0.24	...	0.73 ^b	1.29	...

^a From Aller *et al.* 1987.

^b Assume He/H = 0.09.

^c Measured well above 20000; value adopted from I($\lambda 4686$).

$\lambda 5754$ and sometimes none even on $[\text{O III}] \lambda 4363$ needed for electron temperature determination, nor on the $[\text{O II}]$ or $[\text{S II}]$ doublet ratios used to find electron densities, all of which are critical for the evaluation of accurate compositions. Kaler (1986) calibrated both T_e $[\text{O III}]$ and T_e $[\text{N II}]$ against $I(\lambda 4686)$, so that they could be estimated when the requisite data are missing. However, these relations pertain to the Galaxy with its higher O/H ratio. The lower oxygen abundances of the Clouds will cause higher temperatures. We used Kaler's (1986) correlations between T_e and O/H and also calculated T_e $[\text{N II}]$ for the other (optically thin) nebulae in the Table 1 citation list in order to determine the correction of the T_e $[\lambda 4686]$ relations to the Clouds. We adopt T_e $[\text{N II}] = 11,300$ and $12,400$ K for the LMC and SMC where $I(\lambda 4686) > 10$, and otherwise increase the temperatures (above Kaler's relation) by 10% and 20%, respectively. The final electron temperatures (averaged from individual sources where applicable) are presented in columns (2) and (3) of Table 2. Values derived from $I(\lambda 4686)$ are set into parentheses.

The electron densities require some further innovation. For the bright SMP objects, $[\text{O II}]$ densities are available from MBC (which includes those from Barlow 1987), and from Dopita *et al.* (1988). In a few cases $[\text{S II}]$ densities are available directly from the observations used here, but in two instances are very discordant, so that we only present them, but do not use them directly in the abundance calculations. However, for a pair of SMP nebulae, and for all those with LMC and SMC numbers, no doublet ratios are available, and we must make do with estimates. These objects—even those from BL alone—cover a wide range of evolutionary status; we cannot just use a simple mean. Since the objects are all either entering or are on descending evolutionary tracks, the diameters of the nebulae, and consequently the electron densities, should be roughly correlated to stellar luminosity. In Figure 3 we plot $\log N_e$ from Table 2 against $\log(L_*/L_\odot)$ from Table 1 as open symbols (circles for $[\text{O II}]$, boxes for $[\text{S II}]$). By themselves, the LMC/SMC data define only a slight trend, since those with measured doublet ratios tend to be bright and similar. To these data we add information from KSK, which treats the large

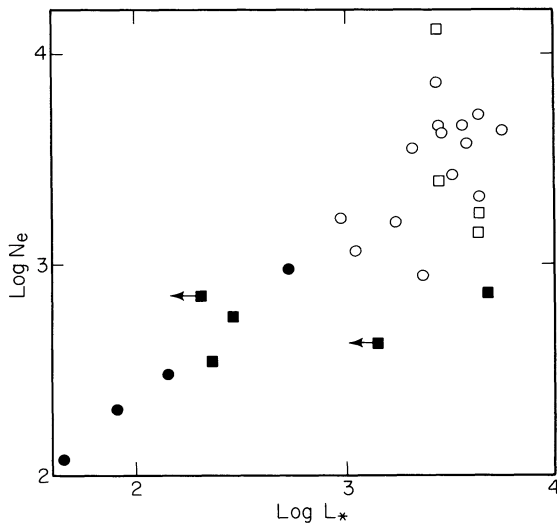


FIG. 3.—The log of nebular electron density plotted against the log of luminosity of the central star. Circles: densities from $[\text{O II}]$, boxes: from $[\text{S II}]$; open symbols: Cloud objects from this paper (Tables 1 and 2); closed symbols: galactic objects from KSK.

galactic nebulae with fainter stars; these are shown as filled symbols, and now define a very nice relationship. We pass an eye-estimate fit to the points and derive N_e from $\log(L_*/L_\odot)$ where necessary and place the results in parentheses in column (4) of Table 2. Below $\log N_e = 3$, the abundances are not very dependent on the exact values and further precision is unwarranted.

The results of the calculations are presented in columns (6) through (12) of Table 2, where ionic ratios are given first, and the three total ratios (He/H, O/H, and N/O) given last. O/H is dependent upon the $\text{He}^{+2}/\text{He}^+$ ratio, and should be viewed skeptically if the latter is above unity. If He^+/H^+ is unknown, but $\text{He}^{+2}/\text{H}^+$ is low, we can reliably estimate total O/H by just adopting a mean He/H.

Errors are difficult to evaluate, since none has been assigned to the observations. For He^+/H^+ we at least can compare the individual values derived from the three He I lines where they are available. As a general rule they are within about 10% of the mean. The $\lambda 4686$ line is strong and close to $\text{H}\beta$, so the error to $\text{He}^{+2}/\text{H}^+$ will be small, probably no greater than 10% as noted earlier. Errors in extinction, temperature, and density are not great factors. Thus the total error to be applied to He/H ought to be around $\pm 10\%$ or ± 0.01 . One exception is SMP 93 for which the $\lambda 4471$ and $\lambda 5876$ lines give discordant results, with an error of nearly 30%.

N/O presents different problems. $[\text{N II}] \lambda 6584$ is so strong and close to $\text{H}\alpha$ that errors in the observations are not very significant. The real problem is in the densities and temperatures. We believe the densities—even the ones derived from the correlation between $\log N_e$ and $\log L_*$ —are realistic. At the higher density end an error of 2000 cm^{-3} produces an error in N/O of perhaps 20% or so. Electron temperature uncertainties are more serious. If the $[\text{N II}]$ auroral line is actually observed, then the effect is trivial. But if we had to adopt T_e $[\text{N II}]$ based on $I(\lambda 4686)$ it could be substantial. Raising T_e $[\text{N II}]$ from 11,300 K—the standard we use for the LMC—to 15,300 K, which probably encompasses the range of error, N/O can climb by around 50% (it is unlikely that T_e would go much below 10,000 K or so). Keep in mind then that some of the N/O values derived from T_e $[\text{N II}]$ in parentheses may be subject to that large an error.

We put little emphasis on O/H here, and use it mostly as a control on errors in T_e . The mean O/H calculated for our LMC objects is 3.49×10^{-4} , 36% higher than that cited above for H II regions, which may reflect errors in electron temperatures or basic procedure. For three nebulae, however—LMC 16, 23, and, 32—O/H is quite anomalous. If we raise the electron temperatures (which have not been measured) for these three objects to 13,000 K, 16,000 K, and 13,000 K, respectively (debatable for T_e $[\text{N II}]$) we can depress the O/H to the above mean, at which point N/O = 0.16, 1.10, and 1.24, respectively.

As an interesting check on the results we plot T_e $[\text{O III}]$ against $\log T_*$ in Figure 4. These two quantities are derived entirely independently of one another, yet the points correlate qualitatively as the temperature of the star (and the energy input into the nebula) increases, so does the nebular electron temperature. The large scatter in T_e $[\text{O III}]$ then correlates with O/H. The dashed line in Figure 4 is a simple eye-estimate fit to the open LMC points. In Figure 5, we plot O/H versus $\Delta T = T_e$ $[\text{O III}]$ (observed) minus the value anticipated from $\log T_*$. As O/H (and the nebular cooling rate) declines, ΔT increases, again as expected; the three SMC objects plotted follow the same trend as do those of the LMC. It appears that real varia-

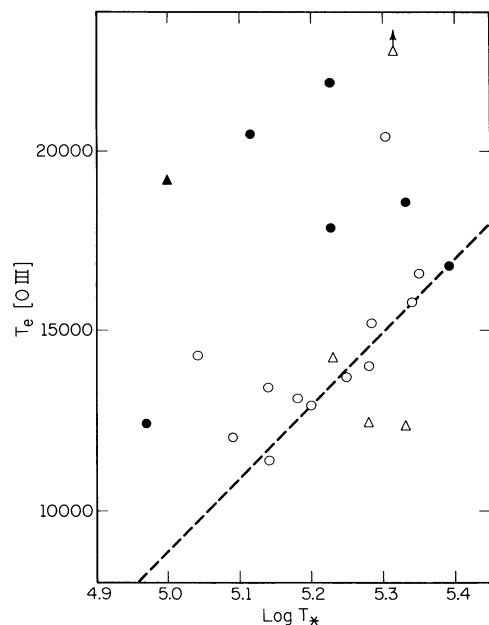


FIG. 4.—The [O III] electron temperatures of the nebulae plotted against the logarithms of the central star temperatures. *Circles*: LMC; *triangles*: SMC; *closed symbols*: data from BL. The dashed line is an eye-estimate fit to the open LMC points.

tions in O/H exist; alternatively, the variation in O/H could reflect errors in $T_e[\text{O III}]$ (or in the simple two-temperature model used). However, the calculated parameters all behave as expected. In the absence of external evidence for errors in T_e , the behavior of the calculated parameters lends credence to the results.

IV. COMPOSITION AND CORE MASS

Now we simply plot N/O against M_c as circles and triangles (depending on the galaxy) in Figures 6 and 7. We also discriminate the objects for which BL fluxes were used by filling in the symbols. In Figure 6 we show the entire range of data. Then for clarity we plot the same data in an expanded version to show the region of lower core mass. (The C/O, plotted on the same

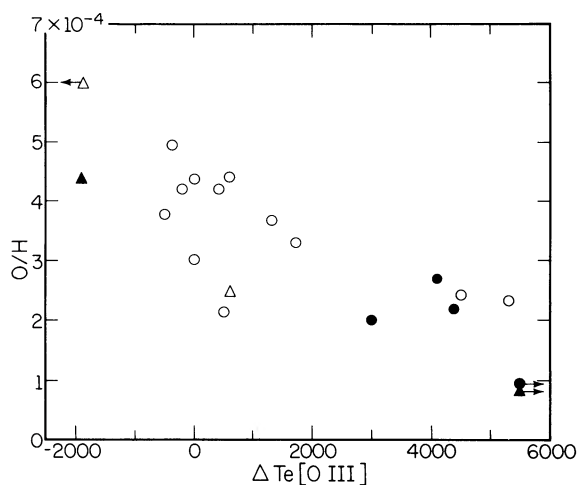


FIG. 5.—O/H from Table 2 plotted against the difference between the observed [O III] electron temperature and that anticipated on the basis of $\log T_*$ and the dashed line in Fig. 4, $\Delta T_e[\text{O III}]$. *Circles*: LMC; *triangles*: SMC. The closed symbols indicate that the data are from BL.

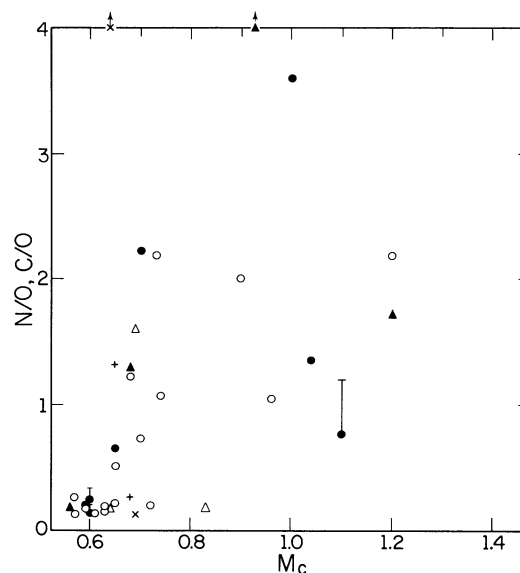


FIG. 6.—Observed N/O (and C/O) from Table 2 plotted against core mass, M_c , from Table 1. *Circles*: LMC; *triangles*: SMC; *closed symbols*: M_c from BL data. The upward bars on these points show how N/O is elevated if T_e is raised so as to reduce the anomalously high O/H values to the average value. The crosses denote C/O from the LMC, the Xs C/O from the SMC.

graphs, are discussed below). The results are quite remarkable and dramatic. Below $0.65 M_\odot$, N/O is roughly constant, with a mean of about 0.18, 5 times that found for Cloud H II regions (Pagel *et al.* 1978; Dufour, Shields, and Talbot 1982); the LMC and the two SMC objects give the same result. (Other authors, e.g. Henry, Liebert, and Boroson 1989; Aller *et al.* 1987, also show that the minimum N/O is high compared to diffuse nebulae). Then at about $0.65 M_\odot$, N/O climbs precipitously with increasing M_c , so that by $0.7 M_\odot$ the N/O is over 2; we show exactly at what core mass large enrichment begins to occur. Remarkably, the admittedly few SMC objects (*triangles*) follow the LMC (*circles*) correlation almost perfectly. The two Clouds appear to behave the same in spite of the difference in initial metallicity.

The sample is too sparse to define clearly the relationship beyond about $0.9 M_\odot$. The figures suggest that the sharp rise

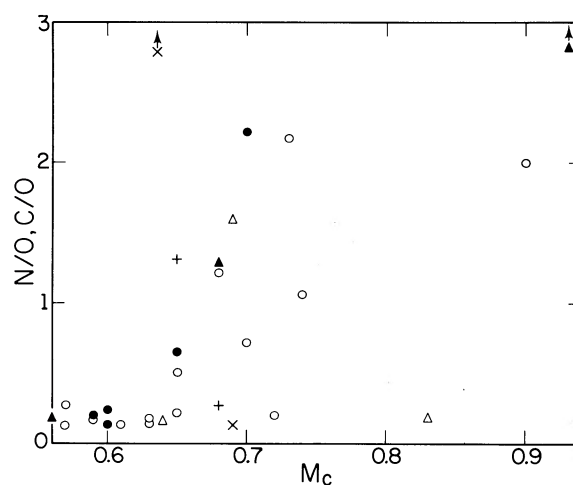


FIG. 7.—N/O (and C/O) plotted against core mass for $0.55 < M_c < 0.95$. This figure is the same as Fig. 6, but expanded to show detail and the nature of the sudden rise of N/O.

represents an envelope. Below $0.65 M_{\odot}$ nitrogen enrichment is fairly constant for all nebulae regardless of core mass. Above the critical mass value, N/O may climb up to a limit, but for individual objects nitrogen enrichment may also stop short of that limit. Interestingly, the highest N/O occur at intermediate M_c , around 0.9 or $1 M_{\odot}$; above $1 M_{\odot}$ the values are lower. This could be a real effect, or it could be caused by too few high-mass data points or by errors in the fluxes.

It is well known that high He/H and high N/O tend to go hand-in-hand (see § I and Henry, Liebert, and Boroson 1989), so we would also expect a correlation between He/H and M_c . These quantities are plotted in Figure 8, where the closed symbols again reflect the use of BL fluxes. Below $0.8 M_{\odot}$, we again see a strong correlation, but now with He/H increasing smoothly with M_c . There seems to be no obviously critical value above which He/H increases, although such might be buried within the scatter: recall that the error is of the order of ± 0.01 , similar to the observed dispersion. The four higher mass stars do not fit the relation and scatter off to the right, much as do the objects with higher mass cores in Figure 6.

Finally, we compare N/O directly with He/H in Figure 9, where those with M_c below and above $0.8 M_{\odot}$ are respectively shown by open and closed symbols. For the set of lower mass cores there is the same sort of rise seen in Figures 6 and 7. There are limited data on those of higher mass, but at elevated N/O they appear to follow their own correlation parallel to and to the left of the main (lower mass) correlation.

The N/O result is consistent with that found by KSK for the Galaxy. KSK's relation is reproduced here for direct comparison in Figure 10. Again we see a flat correlation between N/O and M_c (with an average about double that of the Clouds) that seems suddenly to jump, almost as a step-function, at around 0.7 or $0.8 M_{\odot}$: the large majority of the high N/O objects are at high M_c . We also see that the maximum N/O may occur at intermediate core mass. The difference between the two correlations is probably simply a matter of *distances*. The core masses of the galactic nebulae are found by using the Shklovsky distance method, an uncertain statistical procedure in which we assume that all nebulae have the same mass. The errors for individual objects are likely to be quite large. In

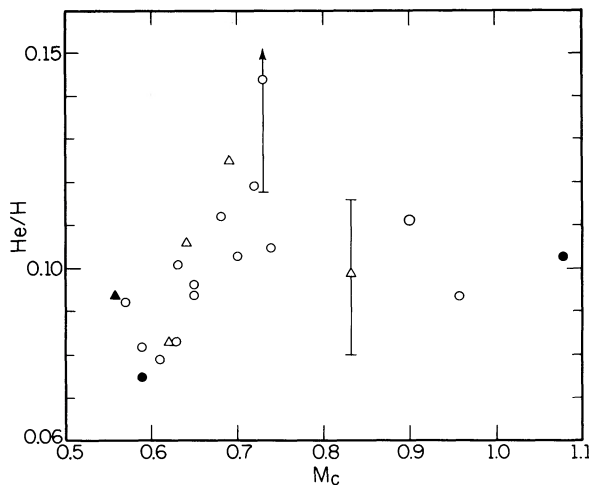


FIG. 8.—He/H from Table 2 plotted against core mass, M_c , from Table 1. Circles: LMC; triangles: SMC; closed symbols: fainter objects with core mass derived from BL. Error bars are placed on two objects for which He/H is particularly uncertain: SMP (LMC) 93 and SMC 3.

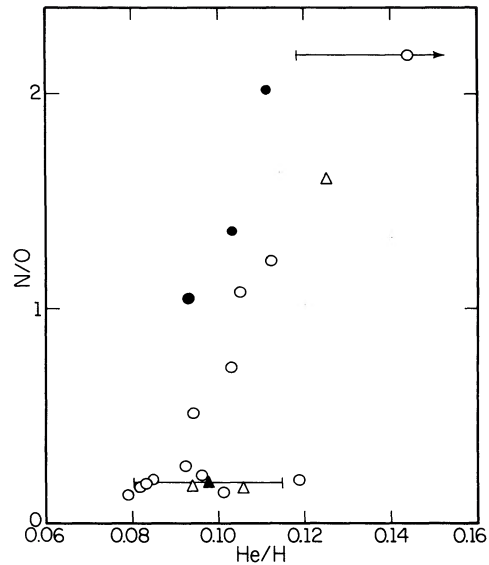


FIG. 9.—N/O plotted against He/H from Table 1. The filled symbols indicate $M_c > 0.8$. He/H error bars are again placed on SMP (LMC) 93 and SMC 3.

addition, many of the KSK nebulae are optically thick, which yields only lower limits to the distances and (since their stars are on descending tracks) to the core masses. If we mentally smear Figure 6 for the Clouds by, say, ± 0.1 in core mass (roughly corresponding to an error of a factor of 3 in distance) we would get something like the KSK relation in Figure 10. Once we know the all-important distances (and use the best available estimates for nebular temperatures and densities where measured values are lacking) the true correlation suddenly appears out of the confusion.

There are yet some deficiencies in the present study. First,

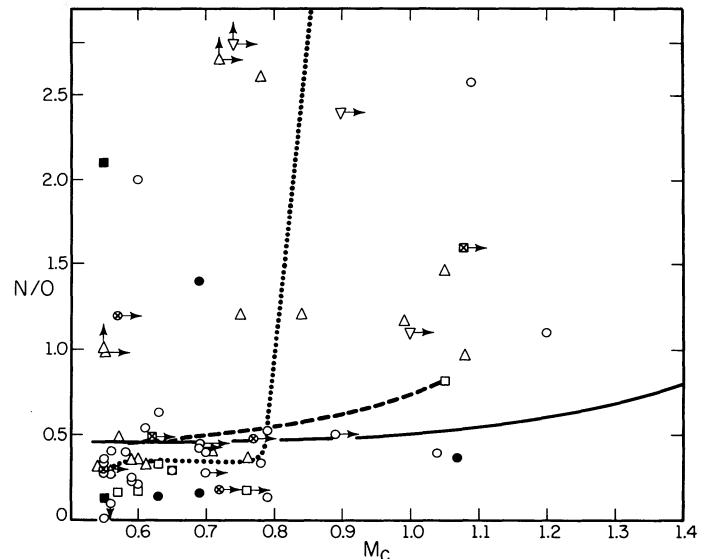


FIG. 10.—N/O plotted against core mass for galactic planetaries taken from Kaler, Shaw, and Kwitter (1990). The solid line shows the correlation expected according to the dredge-up theory of Becker and Iben (1980) (third dredge-up with C to N conversion) and the mass-loss rates of Iben and Truran (1978); the dashed line shows Becker and Iben's theory with Kwok's (1985) mass loss, and the dotted line Renzini and Voli's (1981) envelope-burning for $\alpha = 2$ and Kwok's mass loss.

none of the nebulae on the flat part of the correlation, that below $0.65 M_{\odot}$, has measured $T_e[\text{N II}]$. Since nitrogen is not particularly overabundant the lines are weak and $[\text{N II}]\lambda 5754$ is not observed. However, those eight objects that *do* have $T_e[\text{N II}]$ nicely define the upward slope above $0.65 M_{\odot}$. Second, the $H\beta$ fluxes for the high mass objects are uncertain; and there are just too few high mass optically thick objects, so that in any case it is difficult to define properly the nature of N/O among them. Does N/O really drop above $0.9\text{--}1 M_{\odot}$, or does the upward sweep near $0.7 M_{\odot}$ define an envelope? It will be difficult to increase the sample in order to answer this question. Third, the observations of He/H are rather limited. The variation in helium is much less than that in nitrogen, and more precision is required. It is not really possible to say whether or not the slope of He/H with M_c below $0.8 M_{\odot}$ is linear or contains a break of some sort. Fourth, and perhaps of most importance, is the uncertainty in the $\lambda 3727$ depth criterion (§ II). Several of the *LMC* and all but two of the *SMC* nebulae have $I(\lambda 3727)$ below the conservative galactic criterion of 150. If a nebula is actually optically thin, we will overestimate T_* , underestimate L_* , and consequently overestimate the core mass. However, if we remove all those with $I(\lambda 3727) \lesssim 150$ (keeping SMP 21 and 45 in the *LMC*), the correlation is unaffected. If we adopt the intermediate standards of 120 and 75 for the *LMC* and *SMC* we reject the same number of *LMC* objects but retain all but two of the *SMC* (see Table 1). There is some evidence from Figure 8 that the *LMC* objects with $I(\lambda 3727) < 150$ are systematically found on the right-hand side of the correlation as might be expected. The effect does not seem to be great, however. In summary we feel that there is no question about our having defined clear relationships between composition and core mass, ones that lend themselves well to theoretical analysis.

V. DISCUSSION

First, look at these results just from an empirical point of view. Our observations show broad agreement with those found for giant stars, from which the planetaries evolve. For example, Dickens, Bell, and Gustafsson (1979) find that in the globular cluster 47 Tucanae (which may be an apt comparison object for the Clouds because of depressed metallicity) nitrogen in giants is enriched by about a factor of 5, similar to that found here for core masses between 0.55 and $0.65 M_{\odot}$. The evolving cluster stars all have low mass, of the order of $0.8\text{--}1 M_{\odot}$, and would be expected to evolve into this low core-mass range. Lambert and Ries (1981), however, find N/O ratios of the order of 1 or 2 for field giants, similar to our and KSK's large N/O ratios with intermediate ($0.7\text{--}0.9 M_{\odot}$) core masses. These stars have a range of initial masses and would have higher ultimate core masses than the globular cluster stars.

Figures 6 through 10 provide data on three different galaxies, and ideally the comparisons of the nebulae should tell how enrichment of giant star envelopes depend upon initial conditions. Unfortunately some data are still quite limited. There are only seven *SMC* objects. However, the results for the *SMC* fit quite nicely to those of the *LMC*. There is only one *SMC* object on the flat portion of Figures 6 and 7 ($0.55\text{--}0.65 M_{\odot}$), but it is consistent with the *LMC* nebulae, and three objects on the rising portion ($0.65\text{--}0.95 M_{\odot}$) fit well with their *LMC* counterparts. Perhaps the agreement is not too surprising since even though the O/H in the two galaxies are different, the initial N/O are rather similar (Pagel *et al.* 1978;

Dufour, Shields, and Talbot 1982). Only three *SMC* nebulae have measured He/H, but again they fit with those derived for the *LMC*. Comparison to the Galaxy, which has higher initial O/H, N/O, and He/H, is confounded by distance problems. The median galactic N/O of the flat portion, $0.55\text{--}0.8 M_{\odot}$ (excluding Type I nebulae), is about 0.3, clearly higher (roughly double) than that of the Cloud nebulae. With a solar N/O of 0.15 (Ross and Aller 1976), the low-mass enrichment for galactic objects is only a factor of 2, but for Cloud objects is a factor of 6. Oddly, the final abundances seem to be relatively independent of the initial compositions.

The exact point at which N/O rises for Galactic objects is very confused because of the uncertain distances. KSK suggested that it begins at about $0.7\text{--}0.8 M_{\odot}$. Comparison of Figures 6 and 10 do suggest that the critical core mass may be higher in the Galaxy. That may be due to distance uncertainties and too few objects, to a real metallicity effect, or to an error in the Shklovsky distance scale. KSK used the Cahn and Kaler (1971) scale; if we were to increase distances by 45% or so, as suggested by Méndez *et al.* (1988), then the luminosities would be raised by a factor of 2, and the core masses decreased for descending (cooling) nuclei by roughly $0.1 M_{\odot}$ at $0.7 M_{\odot}$. The matter must for now remain unresolved.

Another intriguing point of comparison is the behavior of N/O above $1 M_{\odot}$. Maximum N/O is reached in the Clouds around 0.9 to $1 M_{\odot}$ (based on only two points). The five with M_c above $1 M_{\odot}$, though still quite enriched, have much lower N/O, on the whole even under those between 0.7 and $0.9 M_{\odot}$. If we add *LMC* 20 at $M_c = 0.96$ and $\text{N/O} = 1.05$ to this group, the six points define their own rising correlation, which may even include the discrepant *SMC* 3 at $M_c = 0.83$, $\text{N/O} = 0.14$. There are really too few points to prove the reality of the effect, but interestingly, in spite of the poor distances, we see a suggestion of the same effect in the Galaxy from KSK's work as shown in Figure 10: the highest N/O tend to occur between 0.7 and $0.9 M_{\odot}$. In addition, He/H shows a similar effect (Fig. 8) as pointed out in the last section. Low and high mass domains may behave differently where the enrichment is less at higher masses, and if we discount observational error, nitrogen is somewhat more enriched relative to helium at high mass than at low (Fig. 9). We will not know whether these effects are real without a great deal more information.

It would also be very interesting to look in detail at carbon abundances for all these objects. Unfortunately there are only four values available, from Aller *et al.* (1987), two in the *LMC* and two in the *SMC* (given in col. [3] of Table 2). They are plotted as crosses and X's respectively in Figures 6 and 7. Henry, Liebert, and Boroson (1988) show an anticorrelation between C/O and N/O; for these four, plotted against core mass, we see the same thing. As N/O rises sharply near $0.65 M_{\odot}$, C/O drops just as quickly, such that (within broad errors) $(\text{C} + \text{N})/\text{O}$ stays relatively constant, implying that the enriched nitrogen is coming from the carbon. The highest values of C/O occurs at relatively low core mass, about $0.64 M_{\odot}$, in agreement with current ideas of carbon star evolution: that a high atmospheric carbon content in *AGB* stars occurs for intermediate initial masses. The carbon stars are confined to an absolute magnitude range of $-4 < M_{\text{bol}} < -6$, which corresponds to C-O core masses between 0.5 and $0.55 M_{\odot}$, comparable to what we see here (see Iben 1988 for a review of this matter and an extensive list of citations). The agreement here between the stars and the planetaries is very satisfying—would that we had C/O data on nebulae of lower core mass so that we could determine where the maximum occurs.

Henry, Liebert, and Boroson (1988) also point out an anticorrelation between N/O and O/H in the Clouds, which is also noted to occur in the Galaxy (see KSK and references therein). Our sample is really too small to explore this matter in depth—that is best done with the full set of *MC* observations—yet at least for the *LMC*, where we have more data, we can still see the existence of the anticorrelation (Fig. 11). It appears in both the high and low mass sets. Further investigation is required. O/H is also oddly high in some Cloud planetaries: compare with the mean values that we have adopted here (indicated in Fig. 11). We would expect the highest values of O/H to fall at the means and to go down from there. At least part of the effect could be caused by observational error combined with erroneous temperature adoptions. It seems possible, though, that at least some of the nitrogen is being created from oxygen.

Numerous studies (see § I) have shown that the observed relation between He/H and N/O in planetaries broadly fits the general prediction of theory. That is, we can select a dredge-up theory (e.g., second dredge-up; third dredge-up with some conversion of C to N, etc.) that will more-or-less agree with the average distribution of abundances, even though it will not accommodate the scatter and the extremes. Now, however, we have a new parameter, the core mass, and a far more powerful way of evaluating the current theories. First, since the theoretical predictions are expressed in terms of initial mass, we must adopt a relation between that and final mass. KSK (Fig. 10) showed that Kwok's (1983) conversion fits better than that from Iben and Truran (1978), that is, it gives a higher N/O for a given M_c , so we shall employ it. Figures 6 and 8 are repeated as Figures 12 and 13 but now with various predictions (as in Fig. 10) applied. The dashed curve in Figures 10 and 12 shows Becker and Iben's (1980) prediction for N/O under conditions of third dredge-up with C to N conversion at one-half the maximum rate (their maximum published enrichments). We see that it does not at all account for the form of the sharp rise. However, the dotted curve from Renzini and Voli's (1981) cal-

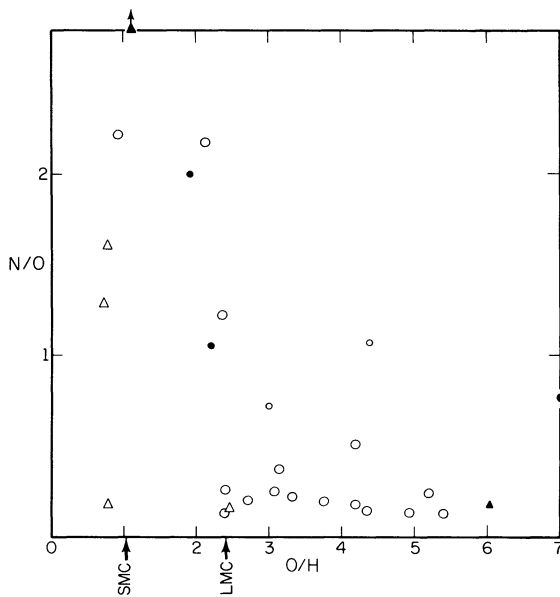


FIG. 11.—N/O plotted against O/H, both from Table 2. Circles: LMC; triangles: SMC. The filled symbols indicate $M_c > 0.8$; the smaller symbols denote $\text{He}^{2+} > \text{He}^+$. The mean O/H for the LMC and SMC (§ II) are indicated by vertical arrows on the lower axis.

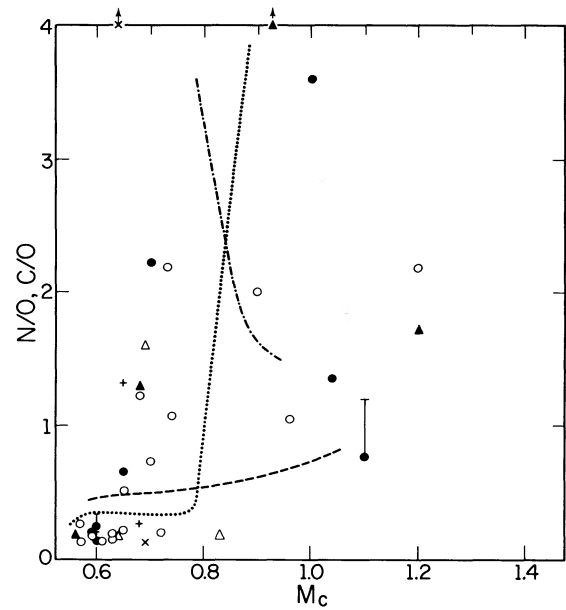


FIG. 12.—The same as Fig. 6 with the Becker-Iben and Renzini-Voli N/O predictions (dashed and dotted lines, respectively) coupled to Kwok's mass-loss rates. The dash-dot curve shows the Renzini-Voli prediction for C/O under envelope-burning conditions.

culations of dredge-up with envelope-burning (with the convective mixing length parameter $\alpha = 2$) fits the form of the rise beautifully, except that it occurs at too high a core mass. The offset could be due to lower metallicity in the Clouds (see above), or could be reconciled by increasing either α or mass-loss rates. We therefore conclude that envelope-burning must play a strong role in giant-star enrichments. However, this curve does not account for the scatter of points to the right, toward higher M_c . As noted in KSK, these are better, if imperfectly, fitted by the Becker and Iben calculations, which employ a lower rate of C to N conversion in the convective zone. Their adopted efficiency of conversion must be increased, however, since the observations of N/O in both the Magellanic Clouds and the Galaxy lie above the prediction. Alternatively, of course, the core masses and/or N/O could be in error.

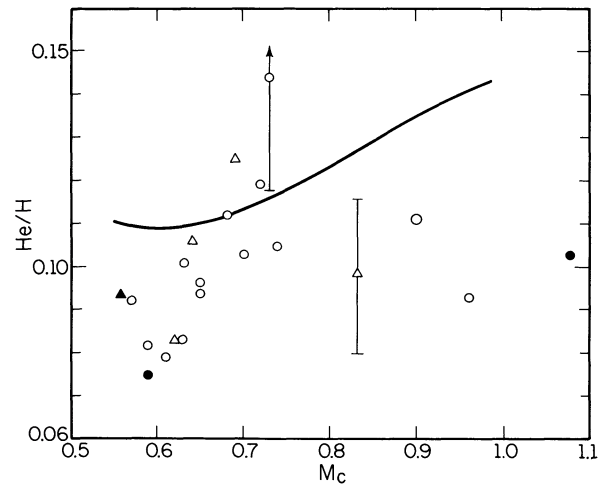


FIG. 13.—The same as Fig. 8 with the theoretical prediction from Becker and Iben and/or Renzini and Voli.

Further supporting the envelope-burning process is the behavior of C/O. The dash-dot curve in Figure 6 shows C/O from the same Renzini-Voli calculations as a function of core mass. It falls steeply, much as do the observations, though again at too high values of M_c ; in addition, it fails by not falling below 1.46. At least the form of the curve appears correct. The theoretical He/H- M_c relation, which is the same for both Becker and Iben and for Renzini and Voli, is shown in Figure 13. It rises at too small a slope relative to the observations below $0.8 M_\odot$, possibly due to lower initial He/H in the Clouds, but more likely because the theory is incorrect in its details.

It appears then that different enrichment processes may be in effect for different mass stars, much as suggested by KSK. Envelope-burning is important for $0.65 < M_c < 1 M_\odot$, corresponding (if Kwok 1983 is correct) to initial masses of $2.25 < M_i < 4.7 M_\odot$. (Remember that this lower core-mass limit—where the onset of nitrogen enrichment occurs—is dependent upon the selection of evolutionary tracks and could be different by the order of 0.05 or so: see § II). The mass for the onset of Peimbert (1978) type I behavior would then be very close to that suggested by Peimbert and Serrano (1980). If that is the case, and if initial metallicity plays no role, then the Renzini-Voli theory should be adjusted by changing α . That, however, is clearly an uncertain conclusion. We then suggest that above a core mass of roughly $1 M_\odot$ envelope-burning has much less of an effect and that enriched nitrogen might be produced more by regular dredge-up processes, or by these plus reduced envelope-burning.

As yet, however, there is no comprehensive theory that will

reproduce what we find here. The final picture will probably include various dredge-up cases in the *RGB* and *AGB* states as well as internal mixing. The observed correlations, however, are now good and precise enough to direct theory; that is, to provide a strict control on theoretical predictions. This control will improve along with the observations. What are needed are: (1) improvement and/or confirmation of H β fluxes for faint objects; (2) more optically thick nebulae (especially in the *SMC*) that will allow the placement of more objects on the ($\log L - \log T$)-plane and the determination of more core masses; (3) measurement of He/H in the fainter *LMC* nebulae and in the *SMC* in general; (4) improvement of the [N II] electron temperatures in order to provide more accurate N/O ratios; (5) a great improvement in the number of C/O ratios for optically thick nebulae; and (6) better distances for galactic objects so as to examine the effects of initial metallicity.

With this work we embark on a serious exploration of how stars dredge up the by-products of thermonuclear burning, wherein we can see how the process—or processes—are related to mass. The ultimate goal is to be able to examine a nebular spectrum and tell where on the main sequence the star originated. Since the planetary nucleus can be directly related to the white dwarfs, the whole path of stellar evolution becomes open, allowing the determination of the relation between initial and final conditions for low- and intermediate-mass stars.

This work was supported by National Science Foundation grant AST 88-13686 to the University of Illinois. We would like to thank Louise Browning for help in organization of the data.

REFERENCES

- Aller, L. H. 1976, *Pub. A.S.P.*, **88**, 574.
 ——— 1983, *Ap. J.*, **273**, 590.
 ——— 1984, *Physics of Thermal Gaseous Nebulae* (Dordrecht: Reidel).
 Aller, L. H., Czyzak, S. J., Craine, E., and Kaler, J. B. 1973, *Ap. J.*, **183**, 509.
 Aller, L. H., Keyes, C. D., Maran, S. P., Gull, T. R., Michalitsianos, A. G., and Stecher, T. P. 1987, *Ap. J.*, **320**, 159.
 Aller, L. H., Keyes, C. D., Ross, J. E., and O'Mara, B. J. 1981, *M.N.R.A.S.*, **194**, 613.
 Aller, L. H., and Menzel, D. H. 1945, *Ap. J.*, **102**, 239.
 Ambartsumyan, V. A. 1932, *Pulkovo Obs. Circ.*, Vol. 8, No. 4.
 Barker, T. 1978, *Ap. J.*, **220**, 193.
 Barlow, M. J. 1987, *M.N.R.A.S.*, **227**, 161.
 Becker, S. A., and Iben, I., Jr. 1979, *Ap. J.*, **232**, 831.
 ——— 1980, *Ap. J.*, **237**, 111.
 Boroson, T. A., and Liebert, J. 1989, *Ap. J.*, **339**, 844 (BL).
 Cahn, J. H., and Kaler, J. B. 1971, *Ap. J. Suppl.*, **23**, 319.
 Clegg, R. E. S. 1987, *M.N.R.A.S.*, **229**, 31p.
 ——— 1989, in *IAU Symposium 131, Planetary Nebulae*, ed. S. Torres-Peimbert (Dordrecht: Reidel), p. 131.
 Conti, P. S., Garmany, C. D., and Massey, P. 1986, *A.J.*, **92**, 48.
 Danziger, I. J., Frogel, J. A., and Persson, S. E. 1973, *Ap. J. (Letters)*, **184**, L29.
 Dickens, R. J., Bell, R. A., and Gustafsson, B. 1979, *Ap. J.*, **232**, 428.
 Dopita, M. A., Ford, H. C., and Webster, B. L. 1985, *Ap. J.*, **297**, 593.
 Dopita, M. A., Meatheringham, S. J., Webster, B. L., and Ford, H. C. 1988, *Ap. J.*, **327**, 639.
 Dufour, R. J., and Killen, R. M. 1977, *Ap. J.*, **211**, 68.
 Dufour, R. J., Shields, G. A., and Talbot, R. J., Jr. 1982, *Ap. J.*, **252**, 461.
 Feast, M. W., and Walker, A. R. 1987, *Ann. Rev. Astr. Ap.*, **25**, 345.
 Greig, W. E. 1971, *Astr. Ap.*, **10**, 161.
 ——— 1972, *Astr. Ap.*, **18**, 70.
 Henry, R. B. C., Liebert, J., and Boroson, T. A. 1989, *Ap. J.*, **339**, 872.
 Henry, R. B. C., and Shipman, H. L. 1986, *Ap. J.*, **311**, 774.
 Iben, I., Jr. 1988, in *Progress and Opportunities in Southern Hemisphere Optical Astronomy (ASP Conf. Ser., No. 1)*, p. 220.
 Iben, I., Jr., and Truran, J. W. 1978, *Ap. J.*, **220**, 980.
 Jacoby, G. H. 1980, *Ap. J. Suppl.*, **42**, 1.
 Jacoby, G. H., and Kaler, J. B. 1989, *A.J.*, **98**, 1662.
 Kaler, J. B. 1974, *Ap. J. (Letters)*, **188**, 215.
 ——— 1976, *Ap. J.*, **210**, 843.
 ——— 1980, *Ap. J.*, **239**, 78.
 ——— 1981, *Ap. J.*, **249**, 201.
 Kaler, J. B. 1983, *Ap. J.*, **271**, 188.
 ——— 1985a, *Ann. Rev. Astr. Ap.*, **23**, 89.
 ——— 1985b, *Ap. J.*, **290**, 531.
 ——— 1986, *Ap. J.*, **308**, 322.
 Kaler, J. B., Iben, I., Jr., and Becker, S. A. 1978, *Ap. J. (Letters)*, **224**, L63.
 Kaler, J. B., and Jacoby, G. H. 1989, *Ap. J.*, **345**, 871 (KJ).
 Kaler, J. B., Shaw, R. A., and Kwitter, K. B. 1989, in *IAU Colloquium 106, Evolution of Peculiar Red Giant Stars*, ed. H. Johnson and B. Zuckerman (Cambridge: Cambridge University Press), p. 235.
 ——— 1990, *Ap. J.*, **359**, 392 (KSK).
 Kwok, S. 1983, in *IAU Symposium 103, Planetary Nebulae*, ed. D. R. Flower (Dordrecht: Reidel), p. 293.
 Lambert, D. L., and Ries, L. M. 1981, *Ap. J.*, **248**, 228.
 Meatheringham, S. J., Dopita, M. A., and Morgan, D. H. 1988, *Ap. J.*, **329**, 166.
 Méndez, R. H., Kudritzki, R. P., Herrero, A., Husfeld, D., and Groth, H. G. 1988, *Astr. Ap.*, **190**, 113.
 Monk, D. J., Barlow, M. J., and Clegg, R. E. S. 1988, *M.N.R.A.S.*, **234**, 583 (MBC).
 Osmer, P. S. 1976, *Ap. J.*, **203**, 352.
 Paczyński, B. 1971, *Acta. Astr.*, **21**, 417.
 Pagel, B. E. J., Edmunds, M. G., Fosbury, R. A. E., and Webster, B. L. 1978, *M.N.R.A.S.*, **184**, 569.
 Peimbert, M. 1978, in *IAU Symposium 76, Planetary Nebulae*, ed. Y. Terzian (Dordrecht: Reidel), p. 215.
 Peimbert, M., and Serrano, A. 1980, *Rev. Mexicana Astr. Ap.*, **5**, 9.
 Peimbert, M., and Torres-Peimbert, S. 1971, *Ap. J.*, **168**, 413.
 Peña, M., and Ruiz, M. T. 1988, *Rev. Mexicana Astr. Ap.*, **16**, 55.
 Pottasch, S. R. 1984, *Planetary Nebulae* (Dordrecht: Reidel).
 Preite-Martinez, A., and Pottasch, S. R. 1983, *Astr. Ap.*, **126**, 31.
 Renzini, A. 1979, in *IAU 4th European Regional Mtg in Astronomy, Stars and Star System*, ed. B. E. Westerlund (Dordrecht: Reidel), p. 155.
 Renzini, A., and Voli, M. 1981, *Astr. Ap.*, **94**, 175.
 Ross, J. A., and Aller, L. H. 1976, *Science*, **191**, 1223.
 Sanduleak, N., MacConnell, D. J., and Philip, A. G. D. 1978, *Pub. A.S.P.*, **90**, 621.
 Shaw, R. A., and Kaler, J. B. 1989, *Ap. J. Suppl.*, **70**, 213.
 Schommer, R. A., Olszewski, E. W., and Aaronson, M. 1984, *Ap. J. (Letters)*, **285**, L53.
 Schönberner, D., and Weidemann, V. 1981, *Physical Process in Red Giants*, ed. I. Iben, Jr. and A. Renzini (Dordrecht: Reidel), p. 463.
 Torres-Peimbert, S., and Peimbert, M. 1978, *Rev. Mexicana Astr. Ap.*, **2**, 1981.

Webster, B. L. 1969, *M.N.R.A.S.*, **143**, 79.

———: 1976, *M.N.R.A.S.*, **174**, 513.

———: 1983, *Pub. A.S.P.*, **95**, 610.

Westerlund, B. E., and Smith, L. F. 1964, *M.N.R.A.S.*, **127**, 449.

Whitford, A. E. 1958, *A.J.*, **63**, 201.

Wood, P. R., and Faulkner, D. J. 1986, *Ap. J.*, **307**, 659.

Wood, P. R., Meatheringham, S. J., Dopita, M. A., and Morgan, D. H. 1987, *Ap. J.*, **320**, 178.

GEORGE H. JACOBY: Kitt Peak National Observatory, National Optical Astronomy Observatories, P.O. Box 26732, Tucson, AZ 85726

JAMES B. KALER: Department of Astronomy, University of Illinois, 103 Astronomy Bldg., 1002 W. Green St., Urbana, IL 61801